

# Corrosion Protection of Carbon Steel in 2M HCl Using *Aizoon canariense* Extract

Abd El-Aziz S.Fouda <sup>1,\*</sup> , Seham M. Abdel Motaal <sup>2</sup>, Amal S. Ahmed <sup>2</sup>, Hayanem B. Sallam <sup>2</sup>, Amira Ezzat <sup>2</sup>, Ahmed El-Hossiany <sup>3</sup>

<sup>1</sup> Department of Chemistry, Faculty of Science, El-Mansoura University, Egypt

<sup>2</sup> Department of Chemistry, Faculty of Science (Girls), Al-Azhar University, Cairo, Egypt

<sup>3</sup> Delta for Fertilizers and Chemical Industries, Talkha, Dakahleya, 1179 Egypt

\* Correspondence: [asfouda@mans.edu.eg](mailto:asfouda@mans.edu.eg);

Scopus Author ID 56231506400

Received: 26.02.2021; Revised: 2.04.2021; Accepted: 7.04.2021; Published: 19.04.2021

**Abstract:** The corrosion inhibition effectiveness of *Aizoon canariense* for carbon steel (CS) in 2 M HCl (the corrosive medium) has been examined by employing chemical and electrochemical methods. The inhibition efficiency was found to improve with a rise in the environment's extract and temperature concentration. The inhibitive effect of this extract was explained on the basis of adsorption on the metal surface; the adsorption effect follows Langmuir adsorption isotherm. The percent inhibition efficiency (IE%) reached 90.23% at 45°C, and activation energy ( $E_a^*$ ) has been determined in the presence and absence of *Aizoon canariense* extract. The corrosion rate was calculated and revealed that *Aizoon canariense* has a good inhibition effect on CS. The surface morphology of CS was examined by employing various techniques. The polarization results indicated that this extract acts as a mixed kind inhibitor. The parameters for the corrosion procedure have also been determined and discussed.

**Keywords:** carbon steel; HCl; carbon steel; Langmuir isotherm; *Aizoon canariense* extract.

© 2021 by the authors. This article is an open-access article distributed under the terms and conditions of the Creative Commons Attribution (CC BY) license (<https://creativecommons.org/licenses/by/4.0/>).

## 1. Introduction

Carbon steel is usually utilized in numerous industries, including building, chemical processing, and oil/gas pipelines, for its low price and unbelievable mechanical properties. Despite all of these properties, CS is highly susceptible to acid attack, especially hydrochloric acid, which is utilized as a cleaner for the surfaces from rust and other scales; this process is known as acid pickling [1]. Inhibitor molecules cover the CS surface and prevent acid from further metal dissolution. The adsorption of inhibitors takes place by two mechanisms; the first is the physisorption, which results from a weak bond due to electrostatic interaction between different charges on the metal surface and inhibitor, the second type is the chemisorption, due to charge electron sharing from the inhibitor molecules to the CS surface to form strong bond [2]. Inhibitors from plant extracts are characterized by their renewable resources, readily obtainable, and don't form any harmful effects on the environment [3]. The green corrosion extracts mainly contain the needful elements (such as O, C, N, and S) that help molecules be adsorbed on the metals or alloys' surface to form a film that protects the surface from dissolution [4]. Table 1 shows some plant extracts' employment as inhibitors to lower steel corrosion in several typical industrial solutions by several authors [5-10].

**Table 1.** List of some plant extracts utilized for the retardation of corrosion of steel.

Plant	Metal	Corrosive medium	%IE	Ref.
Bacopa monnieri	Low carbon steel	0.5M NaOH	80	[5]
Camellia sinensis	Carbon steel	3.5% NaCl	80	[6]
Dioscorea septemloba	Carbon steel	1M HCl	72	[7]
Euphorbia heterophylla Linneo	Mild steel	1.5M HCl	69	[8]
Ipomoea batatas	Galvanized steel	1M HCl	64.26	[9]
Cola acuminata extract	Carbon steel	1M HCl	74	[10]

This research examines the effectiveness of *Aizoon canariense* extract as a corrosion inhibitor for CS in a corrosive acid medium by employing several techniques.

## 2. Materials and Methods

### 2.1. Materials and reagent.

The corrosive acid medium (2 M HCl) was prepared by diluting HCl 37% (a reagent of analytical grade) with bi-distilled water. The composition of the investigated CS as weight % is: C (0.2), Mn (0.37), P (0.026), Si (0.002) and Fe (rest). The CS sheet was mechanically cut into coupons measuring 2×2 x 0.2 cm for weight loss (WL) tests. The samples were abraded with varying degrees of emery papers reaching 1200 grades, cleaned, washed utilizing acetone, and dry with filter paper.

### 2.2. *Aizoon canariense* preparation.

The freshly *Aizoon canariense* parts were firstly prepared to dehydrate, milled to powder. “Then, 500 g of the powder soaked in methanol, boiled at 100°C and preserved at room temperature for about 72 hours. After that, the *Aizoon canariense* is filtrated and put in the air to dry. To attain 1000 ppm stock solution of the extract, one gram from the dried *Aizoon canariense* is dissolved in one liter bi-distilled water. Different concentrations were prepared (50 to 300 ppm) from the stock solution besides the control and were tested for their anti-corrosion effects. Fig. 1 shows chromatographic isolation of the main components of *Aizoon canariense* extracts (1) Leptorumol, (2) Isorhamnetin 7-(6-trans-feruloyl)glucoside, (3) 18-Hydroxy-17-nor-3,16-aphidicolanedione, (4) Seduvioside F, (5) Adenosine, (6) 2,5-Dihydroxy-7-methoxy-6,8-dimethylflavone” [11].

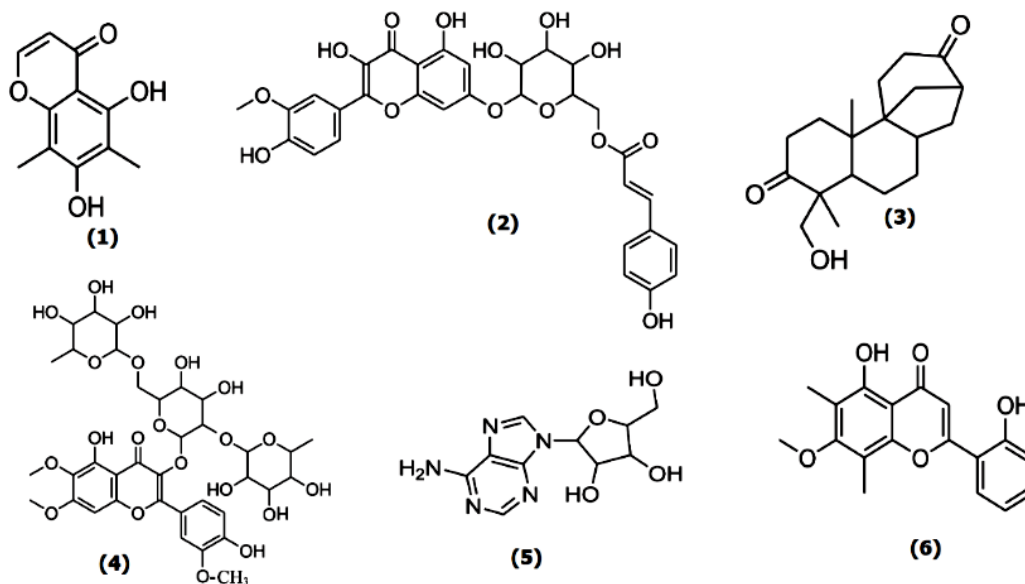


**Figure 1.** Main components in the used *Aizoon canariense* extract.

### 2.3. Weight loss (WL) method.

CS samples with dimensions 2 x 2 x 0.2 cm were prepared as previous and weighted accurately, then suspended in solutions of 100 ml of the corrosive acid medium without and with (50, 100, 150, 200, and 250 ppm) of *Aizoon canariense* for different immersion time (30, 60, 90, 120, 150 and 180 min). The rate of corrosion process ( $k_{\text{corr}}$ ) can be measured as follows:

$$k_{\text{corr}} = \Delta W / At \quad (1)$$

where  $\Delta W$  is WL (mg)  $A$  is the area of CS coins in  $\text{cm}^2$  and  $t$  is the immersion time in min.

### 2.4. Electrochemical techniques.

For electrochemical procedures, a conventional glass cell of three electrodes was employed, with the working electrode (CS), “reference electrode (SCE) and auxiliary electrode (Pt), respectively. For electrochemical tests, we welded the coins with Cu-wire for electrical linking and put them into glass tubes of appropriate diameter utilizing Araldite to offer an active surface of ( $1 \text{ cm}^2$ ) geometric area to contact the test environment. Before each electrochemical test, the CS electrode was dipped for 30 min in the solution to attain a steady-state at open circuit potential. The tests were done utilizing non-stirred 2M HCl with and without altered *Aizoon canariense* extract concentrations as an environmentally friendly corrosion protector. All tests were carried out at  $25 \pm 1^\circ\text{C}$  using a circulator thermostat, and solutions were not deaerated. Electrochemical techniques were carried out using Potentiostat/ Galvanostat (Gamry PCI 300/4) with software DC105, EIS300, and EFM140” for measurements, connected to a computer for data record and store. All the experiments were carried out at  $25^\circ\text{C}$ . Each test was achieved on a newly abraded electrode using a freshly prepared electrolyte.

The potentiodynamic polarization (PP) curves were recorded in the potential range of  $-0.5 \text{ V}$  up to  $+0.5 \text{ V}$  (SCE) relating to the open circuit potential ( $E_{\text{ocp}}$ ) at a rate of a scan of  $1 \text{ mV s}^{-1}$ . The corrosion current density ( $i_{\text{corr}}$ ) was utilized for calculating (%IE).

EIS was recorded at open circuit potential, OCP. The AC signal was 10 mV peak to peak with a frequency range between 100 kHz and 0.1 Hz. %IE and  $\theta$  from both chemical and electrochemical measurements were determine as presented in Table 2:

**Table 2.** Equations utilized to determine the inhibition efficiency.

Technique	Equation
WL [12]	$\% \text{ IE} = \Theta \times 100 = [1 - (W_i / W_0)] \times 100 \quad (2)$
PP [13]	$\% \text{ IE} = \theta \times 100 = [1 - (i_{\text{corr}} / i_{\text{corr}}^0)] \times 100 \quad (3)$
EIS [14]	$\% \text{ IE} = \theta \times 100 = [1 - (R_{\text{ct}}^0 / R_{\text{ct}})] \times 100 \quad (4)$

$W_0$  weight loss values without inhibitor and  $W_i$  with inhibitor;  $i_{\text{corr}}$  and  $i_{\text{corr}}^0$  are the current densities with and without inhibitor; and  $R_{\text{ct}}^0$  and  $R_{\text{ct}}$  are charge transfer resistance values in the absence and presence of the inhibitor, respectively.

### 2.5. Surface analysis.

Atomic force microscope (AFM) and Fourier transform infrared spectroscopy (FT-IR) analysis of “CS surface before and after immersion for 24 hours in the corrosive acid medium without and with 300 ppm (the higher conc.) of *Aizoon canariense* were studied. (AFM) is an effective method employing for examining the surface morphology of CS at nano-to- micro scale. FT-IR spectra were registered in spectral range  $4500$  to  $500 \text{ cm}^{-1}$  with the technique of Attenuated Total Reflectance (ATR) using FTIR-Spectrometer iS 10 (Thermo Fisher Scientific, USA)” [15].

### 3. Results and Discussion

#### 3.1. WL method.

The corrosion method of CS in an aqueous medium is described by the amount to which it dissolves in the solution. “Corrosion rate measurements help to determine the corrosiveness of the studied environment and the rate at which the material is lost by corrosion [16-18]. The conventional method to evaluate the corrosion rate is the WL method. This method evaluates the value of the extract to measure the maximum concentration at which the extract is active in understudied conditions and the surface protecting the ability of the *Aizoon canariense* at high temperatures. Even though the technique is not sophisticated as the optimization of the usage of inhibitor becomes simple through this method”. This method is proved to be the most accurate method to determine the efficiency of the inhibitor (%IE) and the corrosion rate ( $k_{\text{corr}}$ ) (Fig. 2 and Table 3).

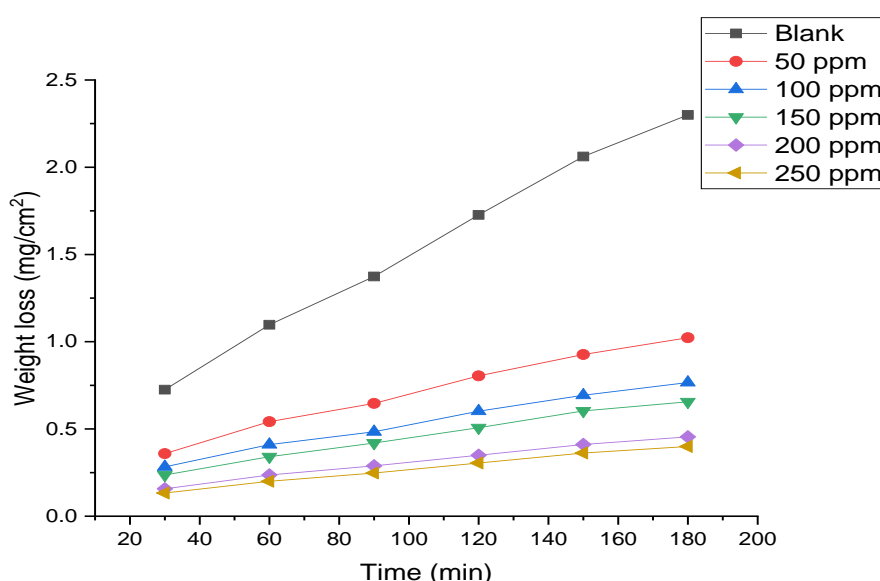


**Figure 2.** WL-time bends for the dissolution of CS in 2 M HCl in the attendance and absence of altered concentrations of *Aizoon canariense* at 25°C.

**Table 3.** Variation of  $k_{\text{corr}}$ ,  $\Theta$ , and %IE for altered concentrations of *Aizoon canariense* at 25 °C.

Conc., ppm	$k_{\text{corr}}$ , $\text{mg cm}^{-2} \text{min}^{-1}$	$\Theta$	%IE
Blank	0.013	--	--
50	0.0057	0.5553	55.53
100	0.004	0.6667	66.67
150	0.0036	0.7149	71.49
200	0.003	0.8023	80.23
250	0.0022	0.8261	82.61

The WL test is usually preferred because the quantity calculated was directly proportional to the dissolution amount. “The Linear variation of WL with time in uninhibited and inhibited aerated acid indicates the absence of insoluble surface films on the metal surface. The *Aizoon canariense* extract is first adsorbed on the CS surface and therefore decreased the corrosion by blocking the active centers (anodic and cathodic)”.

#### 3.2. Effect of temperature.

The influence of temperature on  $k_{\text{corr}}$  and on %IE for CS in the corrosive acid medium without and with altered concentrations of *Aizoon canariense* was analyzed by WL tests in a temperature range from 25 to 45°C. Tables 4, 5 demonstrate that the increase in *Aizoon canariense* concentration decreases  $k_{\text{corr}}$  and increases %IE at all the applied temperatures. This is typically due to the increase of adsorption on the metal surface. The degree of coverage increases with the increase in the *Aizoon canariense* concentration [19]. By raising the *Aizoon canariense* extract temperature, the efficiency increases, demonstrating that *Aizoon canariense* adsorbed on CS surface at these conditions is merely chemical and adsorption.

**Table 4.** The results of WL technique ( $k_{\text{corr}}$  (mg cm<sup>-2</sup> min<sup>-1</sup>),  $\theta$  and % IE) for CS in attendance and absence of *Aizoon canariense* extract after 120 min. at (30, 35°C).

Conc., ppm	30 °C			35 °C		
	$k_{\text{corr}}$	$\theta$	%IE	$k_{\text{corr}}$	$\theta$	%IE
Blank	0.02	---	---	0.033	---	---
50	0.086	0.572	57.2	0.0138	0.5829	58.29
100	0.006	0.6813	68.13	0.01	0.7021	70.21
150	0.0053	0.7379	73.79	0.0083	0.7512	75.12
200	0.004	0.8245	82.45	0.005	0.8463	84.63
250	0.0032	0.8428	84.28	0.0046	0.8629	86.29

**Table 5.** The results of WL technique ( $k_{\text{corr}}$  (mg cm<sup>-2</sup> min<sup>-1</sup>),  $\theta$  and % IE) for CS in attendance and absence of *Aizoon canariense* extract after 120 min. at (40, 45°C).

Conc., ppm	40 °C			45 °C		
	$k_{\text{corr}}$	$\theta$	%IE	$k_{\text{corr}}$	$\theta$	%IE
Blank	0.048	---	---	0.085	---	---
50	0.0193	0.6013	60.13	0.0331	0.6104	61.04
100	0.013	0.7386	73.86	0.021	0.752	75.2
150	0.0106	0.7816	78.16	0.017	0.8001	80.01
200	0.007	0.8627	86.27	0.011	0.8755	87.55
250	0.0059	0.8788	87.88	0.0083	0.9023	90.23

The estimation of activation energies ( $E_a^*$ ) for corrosion of CS in uninhibited and inhibited acid corrosive medium were computed by employing the Arrhenius equation [20]:

$$\log k_{\text{corr}} = -E_a^*/2.303RT + \log A \quad (5)$$

where A is Arrhenius pre-exponential multiplier, T is Kelvin temperature, R is the universal gas constant. Straight lines were obtained by plotting  $\log k_{\text{corr}}$  versus  $1/T$  without and with different concentrations of *Aizoon canariense* (Fig. 3) with slope equals  $(-E_a^*/2.303R)$ . The entropy ( $\Delta S^*$ ) and enthalpy ( $\Delta H^*$ ) of the activation process for CS in the corrosive acid medium without and with different concentrations of *Aizoon canariense* were computed by employing the next transition-state equation [21]:

$$k_{\text{corr}} = RT/Nh \exp(\Delta S^*/R) \exp(-\Delta H^*/RT) \quad (6)$$

where “N & h represents Avogadro’s number and Planck’s constant, respectively. Straight lines were obtained by plotting  $\log k_{\text{corr}}/T$  versus  $1/T$  without and with an altered concentration of *Aizoon canariense* (Fig. 4) with slope equals  $(-\Delta H^*/2.303R)$ , and the intercept equals  $[(\log(R/Nh) + (\Delta S^*/2.303R))]$ . The computed activation parameters ( $E_a^*$ ,  $\Delta H^*$ , and  $\Delta S^*$ ) were provided in Table 6. The data in Table 6 illustrated that the highest values of  $E_a^*$  and  $\Delta H^*$  are shown in the absence of the *Aizoon canariense*, and this indicates that chemical adsorption of *Aizoon canariense* occurs on the CS surface.  $\Delta H^*$  values have positive signs, which means that the *Aizoon canariense* molecules are adsorbed endothermically on the CS, which confirms the

extract's chemical adsorption on the CS surface. Negative  $\Delta S^*$  values indicate that the activated complex prefers association rather than dissolution" [22, 23].

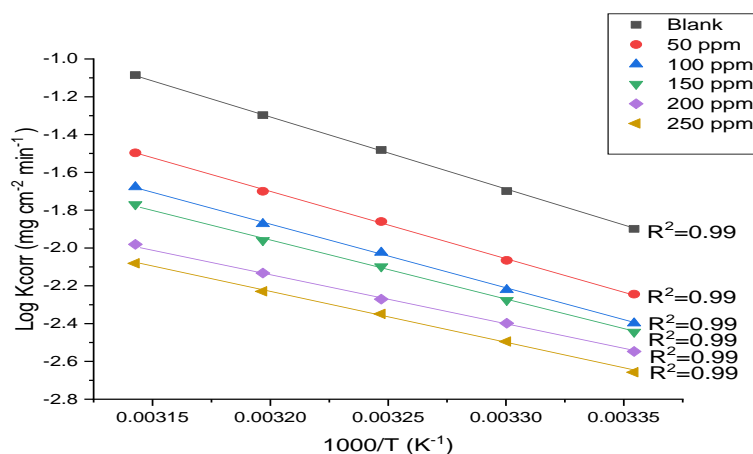


**Figure 3.** Plotting  $\log k_{\text{corr}}$  against  $1/T$  for CS in the attendance and absence of various concentrations of *Aizoon canariense* extract.

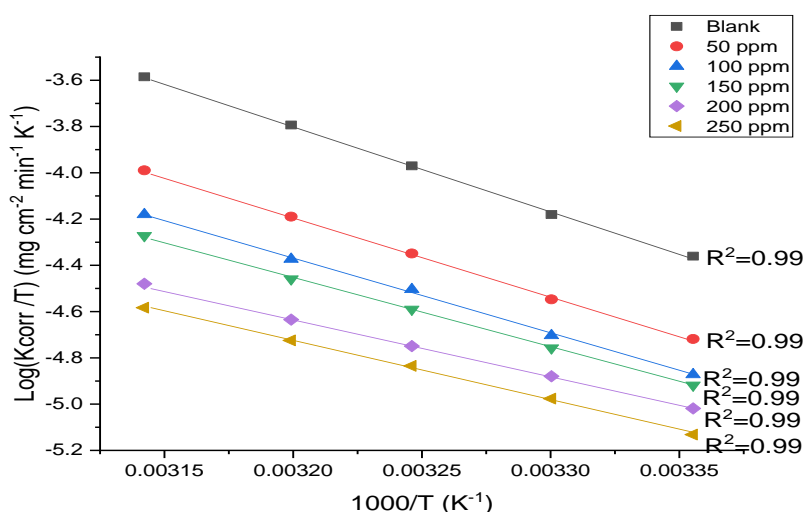


**Figure 4.** Plotting  $\log k_{\text{corr}}/T$  against  $1/T$  for CS in the attendance and absence of various concentrations of *Aizoon canariense* extract.

**Table 6.** Activation parameters ( $E_a^*$ ,  $\Delta H^*$ , and  $\Delta S^*$ ) for CS in the attendance and absence of various concentrations of *Aizoon canariense* extract.

$C_{\text{inh}}$ , ppm	$E_a^*$ , kJ/mol	$\Delta H^*$ , kJ/mol	$-\Delta S^*$ , J/mol.K
Blank	73.66	70.26	45.34
50	67.58	65.86	66.92
100	65.01	62.22	81.97
150	60.48	57.72	97.99
200	50.79	48.10	132.48
250	51.56	48.90	131.26

### 3.3. Adsorption isotherm.

Quantitative expression of adsorption is best described by obtaining the adsorption isotherm that features the metal/inhibitor/environment system. The values of  $\theta$  were estimated at altered extract concentrations in an acidic environment. Tries were made to fit  $\theta$  data to altered adsorption isotherms. The Langmuir isotherm is represented by:

$$C / \theta = 1 / K_{\text{ads}} + C \quad (7)$$

Where  $C$  is the investigated *Aizoon canariense* extract concentration,  $K_{ads}$  is the equilibrium adsorption constant. Plotting of  $C / \theta$  vs.  $C$  for adsorbed *Aizoon canariense* extract on the surface of CS in 2 M HCl acid at altered temperatures were displayed in Fig. 5. The data gave straight lines with a maximum value of correlation coefficient indication that Langmuir isotherm is valid for this system.

In this study,  $\Delta G^0_{ads}$  was used to study the interaction of *Aizoon canariense* molecules, and this was done using the next Eq.:

$$\Delta G^0_{ads} = -RT \ln (55.5 \times K_{ads}) \quad (8)$$

The value 55.5 reveals the concentration of water in the bulk solution where it is expressed in mol/L. “Table 7 shows the adsorption parameters for the obtained *Aizoon canariense* extract. The table's data confirm the spontaneous adsorption of *Aizoon canariense* extract on the CS surface through the negative values obtained  $\Delta G^0_{ads}$ , whose negative value lowered with raising the temperature, which approves that the adsorbed layer is more stable at low temperatures. The values of  $\Delta G^0_{ads}$  are less than 20 kJ / mol are physical adsorption and values between 20-40 kJ mol<sup>-1</sup> confirm mixed adsorption (physical and chemical adsorption), this resembles the results obtained” [24]. The enthalpy of adsorption ( $\Delta H^0_{ads}$ ) was computed utilizing the following Vant Hoff equation:

$$\log K_{ads} = -\Delta H^0_{ads} / 2.303RT + \text{constant} \quad (9)$$

Plotting  $\log K_{ads}$  versus  $1/T$  gives a straight line as shown in Fig. 6. The entropy of adsorption ( $\Delta S^0_{ads}$ ) can be calculated from the next Eq.:

$$\Delta S^0_{ads} = (\Delta H^0_{ads} - \Delta G^0_{ads}) / T \quad (10)$$

The calculated  $\Delta H^0_{ads}$  and  $\Delta S^0_{ads}$  values are listed in Table 7. The negative sign of  $\Delta H^0_{ads}$  points out exothermally adsorption of *Aizoon canariense* on CS surface. The exothermic process can refer to physical or chemical adsorption, but the obtained values determine the adsorption type. The calculated values of  $\Delta S^0_{ads}$  point out that the process of adsorption was accompanied by an entropy decrease (an increase of order).

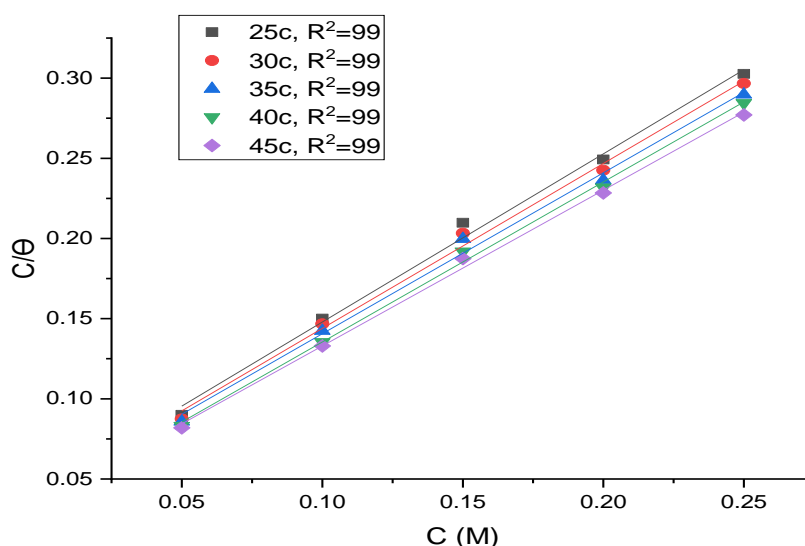


**Figure 5.** Langmuir isotherm of *Aizoon canariense* for dissolution of CS in 2M HCl solution from WL test at altered temperatures.



**Table 7.** Parameters of Langmuir for adsorption of *Aizoon canariense* on the CS surface at altered temperatures.

T, K	$K_{ads} \times 10^{-3}$ $M^{-1}$	$-\Delta G^{\circ}_{ads}$ $kJ\ mol^{-1}$	$\Delta H^{\circ}_{ads}$ $kJ\ mol^{-1}$	$-\Delta S^{\circ}_{ads}$ $J\ mol^{-1}\ K^{-1}$
298	23.25	27.75	17.18	83.64
303	24.34	28.16		83.63
308	24.84	28.51		83.41
313	28.06	29.13		84.05
318	27.90	29.42		83.64

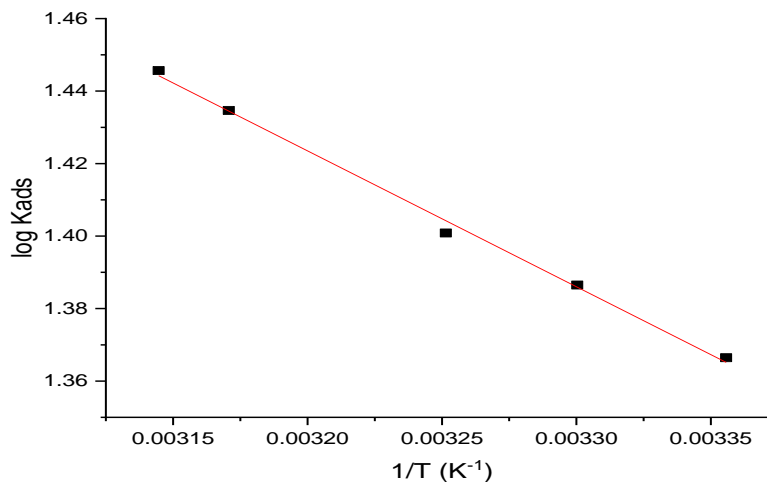


**Figure 6.** Effect of different temperatures on the free energies.

### 3.4. PP tests.

PP diagrams of CS in 2.0 M hydrochloric acid in the existence and absence of altered concentrations of the *Aizoon canariense* extract at 25°C are shown in Fig. 7. “From Fig. 7, we see that both anodic (CS dissolution) and cathodic (hydrogen reduction) reactions were inhibited by adding various concentrations of *Aizoon canariense* extract. Both  $\beta_a$  and  $\beta_c$  were shifted to positive and negative directions, correspondingly. The electrochemical parameters,  $E_{corr}$ ,  $\beta_a$ , and  $\beta_c$ ,  $\theta$ , IE% and  $i_{corr}$  were measured and given in Table 8. Data show that by adding *Aizoon canariense* extract, the values of  $i_{corr}$  were lowered while the values of  $E_{corr}$  and  $\beta_a$  and  $\beta_c$  had no significant change” [25, 26]. So, the *Aizoon canariense* extract acts as a mixed kind inhibitor.

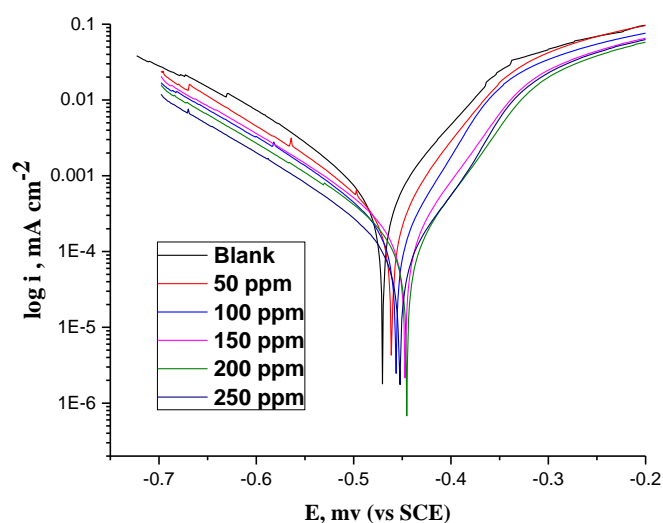


**Figure 7.** The PP curves for the CS dissolution in 2.0 M hydrochloric acid in existence and nonexistence of altered concentrations of *Aizoon canariense* extract at 25°C.



**Table 8.** Electrochemical parameter,  $i_{\text{corr}}$ ,  $E_{\text{corr}}$ ,  $\beta_a$ ,  $\beta_c$ ,  $k_{\text{corr}}$ ,  $\theta$  and IE% of CS in 2 M HCl with altered concentrations of *Aizoon canariense* extract.

Conc., ppm	$-E_{\text{corr}}$ , mV vs SCE	$i_{\text{corr}}$ , $\mu\text{A cm}^{-2}$	$\beta_a$ , mV dec <sup>-1</sup>	$\beta_c$ , mV dec <sup>-1</sup>	C.R., mm y <sup>-1</sup>	$\theta$	% IE
2 M HCl	470	522	72	111	238	----	----
50	461	289	59	108	132	0.446	44.6
100	457	193	61	103	88	0.630	63.0
150	4478	174	66	101	79	0.667	66.7
200	445	139	71	107	63	0.734	73.4
250	453	101	74	97	51	0.807	80.7

### 3.5. EIS test.

“The attained Nyquist, and Bode plots are displayed in Figs. 8, 9 with and without various concentrations of *Aizoon canariense* extract. Nyquist diagrams are represented by a semicircle loop. “These indicate that a charge transfer process governs the corrosion process[27]. The matching circuit that is defined for CS and electrolyte is established in Fig. 10. EIS parameters and % IE were obtained and recorded in Table 9. The results gained in the impedance parameters for CS in 2 M hydrochloric acid in the attendance and absence of *Aizoon canariense* extract's altered concentrations are compiled in Table 9. Figs. 8, 9 show the region of low frequency, and in the existence of *Aizoon canariense* extract, the impedance values rise compared to the absence of the *Aizoon canariense* extract, the radius of the circle rises when the concentration of the *Aizoon canariense* extract increases and hence, the charge transfer resistance in corrosion reactions rises. From all the above, there is high resistance established as the result of adsorption of the *Aizoon canariense* extract at the interface CS /solution” [28]. The capacitance of double layer ( $C_{\text{dl}}$ ) data can be estimated from CPE parameter ( $Y_0$  and  $n$ ) and can be calculated from the next balance:

$$C_{\text{dl}} = Y_0 (\omega_{\text{max}})^{n-1} \quad (11)$$

Where  $Y_0$  is the CPE magnitude, and  $n$  is the variance CPE data of the:  $-1 < n < 1$ . “From Table 9 we note a decrease in the values of  $C_{\text{dl}}$  with an increase in the concentration of *Aizoon canariense* extract, due to a decrease in the local dielectric constant and/or increase in the thickness of the electrical double layer [29]. This is due to the adsorption of *Aizoon canariense* molecules on the CS/interface of solution and forming a protective film on the interface of the CS solution”. Table 9 lists the values of parameters like  $R_s$ ,  $R_{\text{ct}}$ , by EIS fitting and the derived parameters  $C_{\text{dl}}$  and IE %.

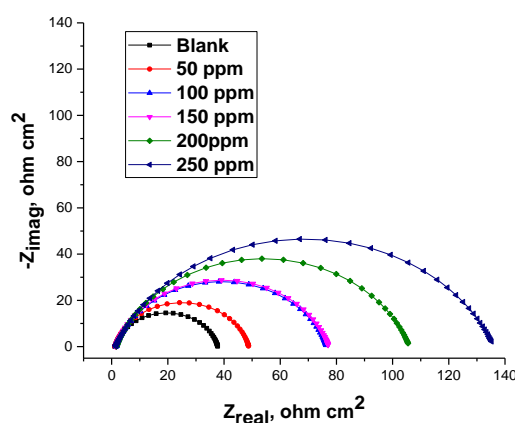


**Figure 8.** The Nyquist plot for CS dissolution in 2M HCl existence and nonexistence of altered *Aizoon canariense* extract concentrations at 25°C.

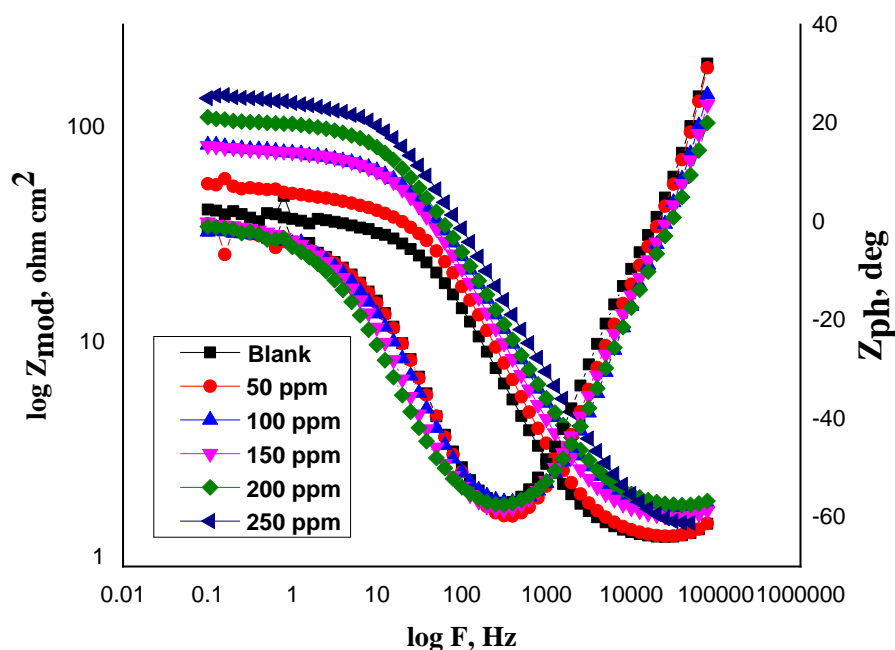


**Figure 9.** The Bode plots for CS dissolution in 2M HCl attendance and absence of altered concentrations of *Aizoon canariense* extract at 25°C.

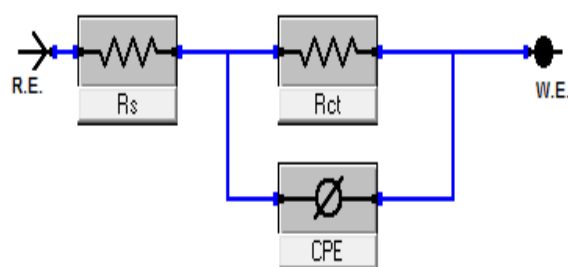


**Figure 10.** The working equivalent circuit for fitting the EIS values.

**Table 9.** Results from EIS tests for the dissolution of CS in 2 M hydrochloric acid at altered concentrations of *Aizoon canariense* extract at 25°C.

Conc., ppm	$Y_o$ , ( $\mu \Omega^{-1} s^n cm^{-2}$ ) $\times 10^{-6}$	n	$R_{ct}$ , $\Omega cm^2$	$C_{dl} \times 10^6$ , $\mu F cm^{-2}$	$\Theta$	% IE
2 M HCl	215.0	0.857	36.5	115	--	--
50 ppm	197.2	0.858	47.5	92	0.232	23.2
100 ppm	181.6	0.819	75.2	70	0.515	51.5
150 ppm	175.4	0.821	77.7	68	0.530	53.0
200ppm	170.2	0.802	104.3	62	0.650	65.0
250 ppm	169.4	0.787	134.8	60	0.729	72.9

### 3.6. Atomic force microscope (AFM) studies.

The CS surface was analyzed using AFM technique after dipping in 2 M HCl in presence and absence of 250 ppm of *Aizoon canariense* extract for 24 h immersion. “The mean roughness profile (Sa) values play an important role in identifying and reporting the extract's efficiency under study [30]. Among the roughness, take a role in explaining the nature of the adsorbed film on the surface. Fig. 11(a) gives the surface of the metal was damaged by HCl (blank) which display high roughness (Sa=1143)” and Fig. 11(b) shows the surface of the C-s in the existence of 250 ppm of *Aizoon canariense*, which does not affect by corrosion and become lower roughness (Sa=133).

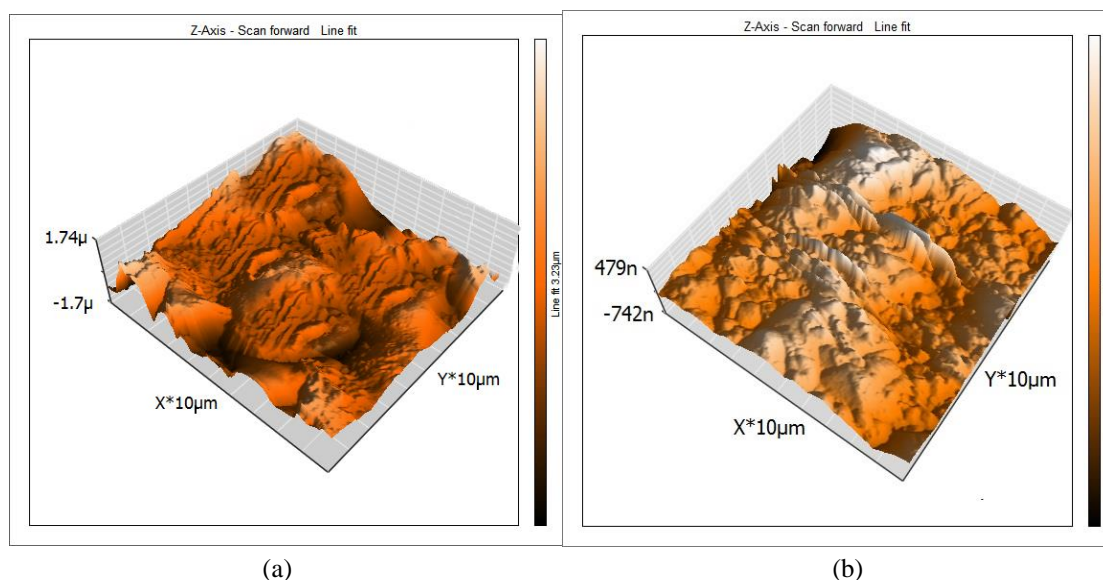


**Figure 11.** (a) Image obtained for the immersion CS specimen in 2 M HCl without *Aizoon canariense* extract and (b) referred to CS specimen after immersion of 2M HCl + 250 ppm of *Aizoon canariense* extracts for 24h.

### 3.7. Fourier transform infrared spectroscopy (FT-IR) analysis.

The FT-IR spectrophotometer is an effective instrument employed for recognizing the functional groups that present in the “*Aizoon canariense* and the type of interaction that occurs between function group and metal surface [31]. Fig. 12 displays broad peaks of *Aizoon canariense* and *Aizoon canariense* with CS. It is clear that there is some peaks displacement between the spectra of the *Aizoon canariense* and the adsorbed extract from CS surface after corrosion; also a few peaks are disappeared or be with less imminent” [32]. This indicates the interaction of *Aizoon canariense* with CS through the functional groups present in *Aizoon canariense* molecules, resulting in the protection from corrosion occurred.

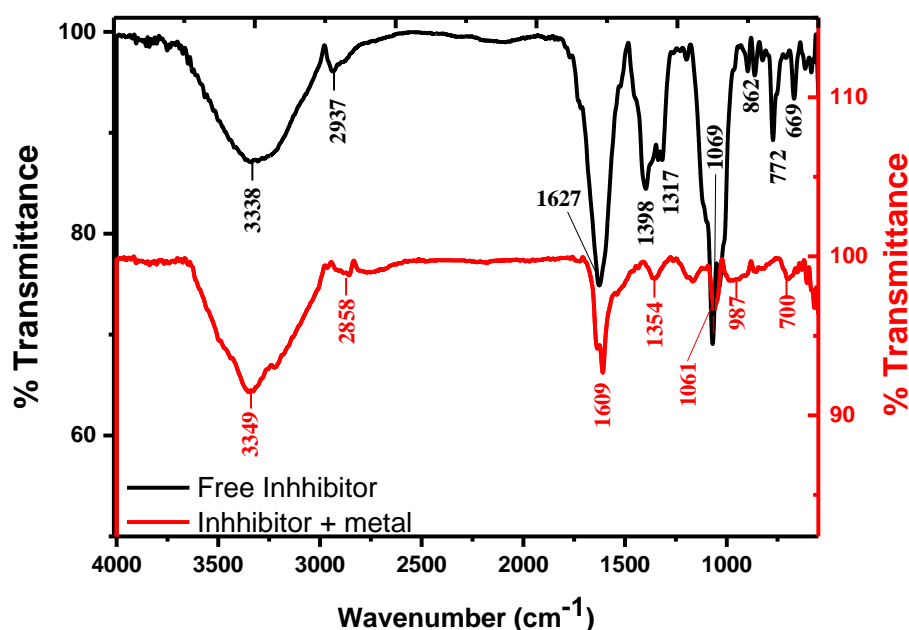


**Figure 12.** FT-IR spectra for *Aizoon canariense* extract only and for *Aizoon canariense* extract adsorbed on CS surface.

### 3.8. Mechanism of corrosion inhibition.

The utilization of *Aizoon canariense* extract as an inhibitor against the corrosion of CS in 2M HCl is due to its adsorption on CS surface Chemically and physically (mixed one). Chemosorption includes the movement of water molecules from the CS surface and sharing of electrons among the vacant d-orbital of CS and oxygen,  $\pi$ - electrons of the aromatic rings present in the extract molecules. In the acid medium CS surface bear's positive charge, it is difficult for the protonated molecules to adsorb on the CS surface due to electrostatic repulsion.  $\text{Cl}^-$  ions get adsorbed on the CS surface, generate an extra negative charge near the solution and approve more adsorption for the cations. It is owing to the electron lone pairs of O and N atoms in *Aizoon canariense* molecules or the protonated molecules may association with freshly produced  $\text{Fe}^{2+}$  ions on the CS surface forming CS inhibitor complexes". These complexes are adsorbed onto the CS by Van Der Waals forces to form protecting cover to prevent CS from corrosion [33, 34]. This *Aizoon canariense* extract will present in the protonated form, so it can adsorb directly on the negative surface of CS in an acidic medium by electrostatic attraction as shown below (Fig. 13):

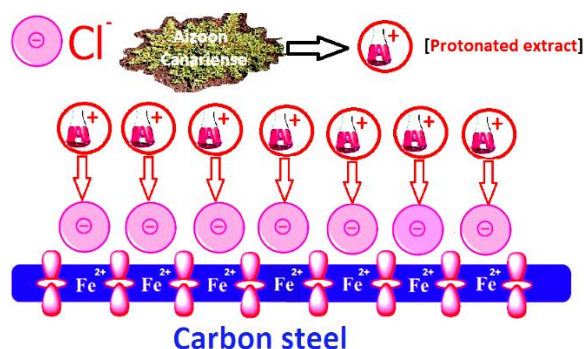


**Figure 13.** Schematic representation of the adsorbed extract molecules on CS surface.

## 4. Conclusions

The influence of *Aizoon canariense* extract as a green corrosion inhibitor for the CS in an aqueous environment utilizing WL test, PP, and EIS techniques have been reported. The WL, PP, and EIS measurements support the assumption that corrosion inhibition primarily occurs through adsorption of the *Aizoon canariense* extracts on the CS surface. The inhibition action improved with increasing both *Aizoon canariense* concentration and temperature. This extract works well at higher temperatures—the adsorption of *Aizoon canariense* on CS surface agreement with Langmuir adsorption isotherm. The values of  $\Delta G^{\circ}_{\text{ads}}$  and  $\Delta H^{\circ}_{\text{ads}}$  estimated from Langmuir isotherm suggest physisorption and chemisorption processes. The adsorbed protective film on the CS surface was confirmed by both AFM and FT-IR techniques. All utilized techniques gave similar results.

## Funding

This research received no external funding.

## Acknowledgments

All our gratitude to the anonymous referees for their careful reading of the manuscript and valuable comments helped shape this paper to the present form. We thank all laboratory staff of corrosion chemistry from the University of Mansoura (Egypt) for their kind cooperation.

## Conflicts of Interest

The authors declare no conflict of interest.

## References

1. Fouda, A.S.; El-Ghaffar, M.A.A.; Sherif, M.H.; El-Habab, A.T.; El-Hossiany, A. Novel Anionic 4-Tert-Octyl Phenol Ethoxylate Phosphate Surfactant as Corrosion Inhibitor for C-steel in Acidic Media. *Protection of Metals and Physical Chemistry of Surfaces* **2020**, *56*, 189-201, <https://doi.org/10.1134/S2070205120010086>.
2. Fouda, A.S.; El-Dossoki, F.I.; El-Hossiany, A.; Sello, E.A. Adsorption and Anticorrosion Behavior of Expired Meloxicam on Mild Steel in Hydrochloric Acid Solution. *Surface Engineering and Applied Electrochemistry* **2020**, *56*, 491-500, <https://doi.org/10.3103/S1068375520040055>.
3. Aoun, S.B.; Messali, M. Microwave-assisted synthesis of green inhibitor for carbon steel acid corrosion. *Int. J. Electrochem. Sci.* **2018**, *13*, 3757–3776, <https://doi.org/10.20964/2018.04.55>.
4. Popoola, L.T. Progress on pharmaceutical drugs, plant extracts and ionic liquids as corrosion inhibitors. *Heliyon* **2019**, *5*, <https://doi.org/10.1016/j.heliyon.2019.e01143>.
5. Al Hasan, N.H.J.; Alaradi, H.J.; Al Mansor, Z.A.K.; Al Shadood, A.H.J. The dual effect of stem extract of Brahmi (*Bacopamonnieri*) and Henna as a green corrosion inhibitor for low carbon steel in 0.5 M NaOH solution. *Case Stud. Constr. Mater.* **2019**, *11*, <https://doi.org/10.1016/j.cscm.2019.e00300>.
6. Pradipta, I.; Kong, D.; Tan, J.B.L. Natural organic antioxidants from green tea inhibit corrosion of steel reinforcing bars embedded in mortar. *Constr. Build. Mater.* **2019**, *227*, <https://doi.org/10.1016/j.conbuildmat.2019.117058>.
7. Emori, W.; Zhang, R.-H.; Okafor, P.C.; Zheng, X.-W.; He, T.; Wei, K.; Lin, X.-Z.; Cheng, C.-R. Adsorption and corrosion inhibition performance of multi-phytoconstituents from *Dioscorea septemloba* on carbon steel in acidic media: Characterization, experimental and theoretical studies. *Colloids Surf. Physicochem. Eng. Asp.* **2020**, *590*, <https://doi.org/10.1016/j.colsurfa.2020.124534>.
8. Akinbulumo, O.A.; Odejebi, O.J.; Odekanle, E.L. Thermodynamics and adsorption study of the corrosion inhibition of mild steel by *Euphorbia heterophylla* L. extract in 1.5 M HCl. *Results Mater.* **2020**, *5*, <https://doi.org/10.1016/j.rinma.2020.100074>.
9. Anyiam, C.K.; Ogbobe, O.; Oguzie, E.E.; Madufor, I.C.; Nwanonenyi, S.C.; Onuegbu, G.C.; Obasi, H.C.; Chidiebere, M.A. Corrosion inhibition of galvanized steel in hydrochloric acid medium by a physically modified starch. *SN Appl. Sci.* **2020**, *2*, <https://doi.org/10.1007/s42452-020-2322-2>.
10. Mohammed, A.R.I.; Solomon, M.M.; Haruna, K.; Umoren, S.A.; Saleh, T.A. Evaluation of the corrosion inhibition efficacy of *Cola acuminata* extract for low carbon steel in simulated acid pickling environment. *Environmental Science and Pollution Research* **2020**, *27*, 34270–34288, <https://doi.org/10.1007/s11356-020-09636-w>.
11. Abuzaid, H.; Amin, E.; Moawad, A.; Abdelmohsen, U.R.; Hetta, M.; Mohammed, R. Liquid chromatography high-resolution mass spectrometry analysis, phytochemical and biological study of two aizoaceae plants: A new kaempferol derivative from *Trianthema portulacastrum* L. *Pharmacognosy Research* **2020**, *12*, 212-218.
12. Haldhar R.; Prasad D.; Bahadur, I.; Dagdag, O.; Berisha, A. Evaluation of *Gloriosa superba* seeds extract as corrosion inhibition for low carbon steel in sulfuric acidic medium: A combined experimental and computational studies, *Journal of Molecular Liquids* **2021**, *323*, 114958–114967, <https://doi.org/10.1016/j.molliq.2020.114958>.
13. Vorobyova, V.; Skiba, M. Peach Pomace Extract as Efficient Sustainable Inhibitor for Carbon Steel Against Chloride-Induced Corrosion. *Journal of Bio-and Tribo-Corrosion* **2021**, *7*, 1–11, <https://doi.org/10.1007/s40735-020-00450-y>.
14. Peñaloza, E.; Holandino, C.; Scherr, C.; de Araujo, P.I.; Borges, R.M.; Urech, K.; Baumgartner, S.; Garrett, R. Comprehensive Metabolome Analysis of Fermented Aqueous Extracts of *Viscum album* L. by Liquid Chromatography– High Resolution Tandem Mass Spectrometry. *Molecules* **2020**, *25*, 4006-4020, <https://doi.org/10.3390/molecules25174006>.
15. Agbaffa, E.B.; Akintemi, E.O.; Uduak, E.A.; Oyeneyin, O.E. Corrosion inhibition potential of the methanolic crude extract of *Mimosa pudica* leaves for mild steel in 1 M hydrochloric acid solution by weight loss method. *Science Letters* **2021**, *15*, 23–42, <https://doi.org/10.24191/sl.v15i1.11791>.



16. Elabbasy, H.M.; Zidan, S.M.; Fouda, A.S. Inhibitive behavior of ambrosia maritima extract as aneco-friendly corrosion inhibitor for carbon steel in 1M HCl. *Zastita Materijala* **2019**, *60*, 129-146, <https://doi.org/10.5937/zasmat1902129E>.
17. Fouda, A.S.; Abd El-Maksoud, S.A.; El-Hossiany, A.; Ibrahim, A. Corrosion Protection of Stainless Steel 201 in Acidic Media using Novel Hydrazine Derivatives as Corrosion Inhibitors. *Int. J. Electrochem. Sci.* **2019**, *14*, 2187-2207, <https://doi.org/10.20964/2019.03.15>.
18. Fouda, A.S.; Al-Hazmi, N.E.; El-Zehry, H.H.; El-Hossainy, A. Electrochemical and Surface Characterization of Chondria Macrocarpa Extract (CME) as Save Corrosion Inhibitor for Aluminum in 1M HCl Medium. *Journal of Applicable Chemistry* **2020**, *9*, 362-381.
19. Raghavendra, N.; Hublikar, L.V.; Patil, S.M.; Ganiger, P.J.; Bhinge, A.S. Efficiency of sapota leaf extract against aluminium corrosion in a 3 M sodium hydroxide hostile fluid atmosphere: a green and sustainable approach. *Bulletin of Materials Science* **2019**, *42*, <https://doi.org/10.1007/s12034-019-1922-1>.
20. Fouda, A.S.; Rashwan, S.; Kamel, M.M.; Arman, N.M. Adsorption and Inhibition Behavior of Avicennia Marina for Zn Metal in Hydrochloric Acid Solution. *International Journal of Electrochemical Science* **2017**, *12*, 11789-11804, <https://doi.org/10.20964/2017.12.95>.
21. Fouda, A.S.; Abd El-Maksoud, S.A.; El-Hossiany, A.; Ibrahim, A. Effectiveness of Some Organic Compounds as Corrosion Inhibitors for Stainless Steel 201 in 1M HCl: Experimental and Theoretical Studies. *Int. J. Electrochem. Sci.* **2018**, *13*, 9826-9846, <https://doi.org/10.20964/2018.10.36>.
22. Ibrahim, M.B.; Sulaiman, Z.; Usman, B.; Ibrahim, M.A. Effect of Henna Leaves on the Corrosion Inhibition of Tin in Acidic and Alkaline Media. *World Journal of Applied Chemistry* **2019**, *4*, 54-51, <https://doi.org/10.11648/j.wjac.20190404.11>.
23. Fouda, A.S.; Abdel Azeem, M.; Mohamed, S.A.; El-Hossiany, A.; El-Desouky, E. Corrosion Inhibition and Adsorption Behavior of Nerium Oleander Extract on Carbon Steel in Hydrochloric Acid Solution. *Int. J. Electrochem. Sci.* **2019**, *14*, 3932-3948, <https://doi.org/10.20964/2019.04.44>.
24. Baymou, Y.; Bidi, H.; Ebn Touhami, M.; Allam, M.; Rkayae, M.; Belakhmima, R.A. Corrosion Protection for Cast Iron in Sulfamic Acid Solutions and Studies of the Cooperative Effect Between Cationic Surfactant and Acid Counterions. *Journal of Bio- and Tribo-Corrosion* **2018**, *4*, <https://doi.org/10.1007/s40735-018-0127-2>.
25. Zhang, S.; Hou, L.; Du, H.; Wei, H.; Liu, B.; Wei, Y. A study on the interaction between chloride ions and CO<sub>2</sub> towards carbon steel corrosion. *Corrosion Science* **2020**, *167*, 108531-108541, <https://doi.org/10.1016/j.corsci.2020.108531>.
26. Fouda, A.S.; Killa, H.M.; Farouk, A.; Salem, A.M. Calicotome Extract as a Friendly Corrosion Inhibitor for Carbon Steel in Polluted NaCl Solution: Chemical and Electrochemical Studies. *Egyptian Journal of Chemistry* **2019**, *62*, 1879-1894, <https://doi.org/10.21608/EJCHEM.2019.7656.1649>.
27. Fouda, A.S.; Eissa, M.; El-Hossiany, A.; Ciprofloxacin as Eco-Friendly Corrosion Inhibitor for Carbon Steel in Hydrochloric Acid Solution. *Int. J. Electrochem. Sci.* **2018**, *13*, 11096-11112, <https://doi.org/10.20964/2018.11.86>.
28. Fouda, A.S.; Rashwan, S.; El-Hossiany, A.; El-Morsy, F.E. Corrosion Inhibition of Zinc in Hydrochloric Acid Solution using some organic compounds as Eco-friendly Inhibitors. *Journal of Chemical, Biological and Physical Sciences* **2019**, *9*, 001-024, <https://doi.org/10.24214/jcbps.A.9.1.00124>.
29. Hsissou, R.; Abbout, S.; Berisha, A.; Berradi, M.; Assouag, M.; Hajjaji, N.; Elharfi, A. Experimental, DFT and molecular dynamics simulation on the inhibition performance of the DGDCBA epoxy polymer against the corrosion of the E24 carbon steel in 1.0 M HCl solution. *Journal of Molecular Structure* **2019**, *1182*, 340-351, <https://doi.org/10.1016/j.molstruc.2018.12.030>.
30. Motawea, M.M.; El-Hossiany, A.; Fouda, A.S. Corrosion Control of Copper in Nitric Acid Solution using Chenopodium Extract. *Int. J. Electrochem. Sci.* **2019**, *14*, 1372-1387, <https://doi.org/10.20964/2019.02.29>.
31. Soltani, N.; Tavakkoli, N.; Attaran, A.; Karimi, B.; Khayat Kashani, M. Inhibitory effect of Pistacia khinjuk aerial part extract for carbon steel corrosion in sulfuric acid and hydrochloric acid solutions. *Chemical Papers* **2020**, *74*, 1799-1815, <https://doi.org/10.1007/s11696-019-01026-y>.
32. Abdel-Gaber, A.M.; Rahal, H.T. and Beqai, F.T. Eucalyptus leaf extract as a eco-friendly corrosion inhibitor for mild steel in sulfuric and phosphoric acid solutions. *International Journal of Industrial Chemistry* **2020**, 1-10, <https://doi.org/10.1007/s40090-020-00207-z>.
33. Haldhar, R.; Prasad, D. and Bhardwaj, N. Extraction and experimental studies of Citrus aurantifolia as an economical and green corrosion inhibitor for mild steel in acidic media. *Journal of Adhesion Science and Technology* **2019**, *33*, 1169-1183, <https://doi.org/10.1080/01694243.2019.1585030>.
34. Fouda, A.S.; Abd El-Maksoud, S.A.; El-Hossiany, A.; Ibrahim, A. Evolution of the Corrosion-inhibiting Efficiency of Novel Hydrazine Derivatives against Corrosion of Stainless Steel 201 in Acidic Medium. *Int. J. Electrochem. Sci.* **2019**, *14*, 6045-6064, <https://doi.org/10.20964/2019.07.65>.